Natural Resources for Human Health
eISSN: 2583-1194

Original Research
Received 15 March 2026
Revised 20 April 2026
Accepted 24 May 2026

Natural Resources for Human Health 2026, Vol. 6 (2s): 246–258

KEYWORDS:
Dermoscopic Image Analysis, Public Awareness, SAID-Net, Skin Cancer Classification, Sun-Safety, Behaviors Melanoma Detection.

Evaluating Public Awareness of Skin Cancer Risk Factors and Adherence to Sun-Safety Behaviors

Nalini S[1], Ramaprabha Jayaram[2], Dr. Vijayakumar N C[3], Dr. Rajarajeswari K[4], Dr. N. Balachandran[5]

[1]Department of Computing Technologies, School of Computing, Faculty of Engineering and Technology, SRM Institute of Science and Technology, Kattankulathur - 603 203, Tamilnadu, India. nalini.tamilmani@gmail.com ORCID: 0000-0003-2393-5848

[2]Department of Computing Technologies, School of Computing, Faculty of Engineering and Technology, SRM Institute of Science and Technology, Kattankulathur -603 203. Tamilnadu, India Mail: ramapraj@srmist.edu.in ORCID: 0000-0002-3304-3176

[3]Associate Professor, School of Business, Alliance University, Bangalore, India. Mail: ncvijayakumar@gmail.com ORCID: 0009-0005-4588-7500

[4]Assistant professor, Center for Management studies, Jain University, Bangalore, India. Mail:drrajarajeswari21@gmai.com ORCID: 0009-0007-2973-3856

[5]Associate Professor, Department of Management Studies (MBA), Velalar College of Engineering and Technology, Erode, Tamil Nadu, India. Mail: nbalachandran55@gmail.com, ORCID: 0000-0001-6318-6808

ABSTRACT: Skin cancer is the most common cancer in the world and is the most common form of cancer reported in the world each year which correlates to a rise in exposure to ultraviolet (UV) radiation and ozone depletion. Although the field of developing deep learning-based diagnostic systems is advancing rapidly, public understanding of the risk factors for skin cancer and practices of sun protection behaviors such as use of sun protection products and sun protection clothing are still lacking. These preventive practices are different in various populations that make it difficult to do real-world intervention. In this research, a hybrid deep learning architecture for multi-class skin lesion classification networks is proposed, Sun Awareness Intelligent Diagnosis Network (SAID-Net), which can explain the diagnosis, to solve both these problems. It incorporates EfficientNetV2, a local feature extractor for texture features, Vision Transformer with Multi-Head Self-Attention (ViT-MHSA), which is a global feature extractor for contextual information and Explainable AI (XAI) Attention module, which identifies and highlights clinically relevant lesion areas for greater transparency during diagnosis. Pre-processing consists of dermoscopic hair removal, image contrast enhancement by CLAHE and normalization of images. Evaluated on the ISIC dataset, SAID-Net achieves 99.12% accuracy, outperforming CNN (92.84%), ResNet50 (94.27%), ASFF (95.36%), LSTM (96.14%) and Denoising Autoencoder (97.03%). The integrated system can be used in detecting skin cancer automatically and can be applied in public campaigns for sun safety.

1. INTRODUCTION

Skin cancer is one of the leading cancers of the world with millions of new cases being diagnosed annually (Panwar et al., 2026). Environmental changes (e.g., ozone depletion and heightened exposure to ultraviolet (UV) radiation) have been associated with the rise in the number of different skin cancers (Tariq et al., 2026). Although much work has been done in the development of deep learning-based skin cancer diagnostic systems, it has led to a significant improvement in the accuracy of early detection (Ajabani et al., 2025), the effectiveness of any skin cancer intervention depends on the preventive practices that are adopted by the population (Saleh et al., 2026).

Sun protection behaviors like using sun protection measures (SPP), wearing protective clothing, staying out of high UV hours and seeking shade are known protective behaviors (Gabani et al., 2026). However, there are no public health policies broadly implemented to ensure compliance, as it is not well adhered in many populations due to lack of awareness of risk factors, perception of exposure to UV radiation and demographic factors (Alamri et al., 2026). Most research on automated diagnostic systems (e.g., LesionNet, Alzakari et al., 2024) has concentrated on technology, while few research have examined the "take home" message of raising public awareness and uptake of behavior change in skin cancer prevention (Zareen et al., 2024).

Medical insurance fraud education is essential for raising awareness among the public, as evidenced by the concerns raised with synthetic images of skin cancer and comprehensive assessments highlight the need for a more holistic approach that combines medical insurance fraud education with diagnostic advances and public health initiatives (Alshmrani et al., 2026; Minarno et al., 2024). The purpose of the research is to assess the awareness of the public on the risk factors of skin cancer, the awareness on the required preventive measures and to compare the performances of the technologies with the community level on the aspects of prevention.

Section 1 provides an overview of the epidemiology of skin cancer, sun-safety behaviours and SAID-Net framework. A background research of existing approaches to deep learning is discussed in Section 2. The description of the data set ISIC and the SAID-Net architecture are given in Section 3. The comparative and ablative evaluation, class-wise evaluation, computational evaluation, explainability evaluation and awareness assessment results are reported in section 4. Section 5 provides discussion and statistical justifications, robustness and implications and limitations.

2. BACKGROUND STUDY

Islam and Panta (2024) provided binary classification of skin cancer by transfer learning of five pre-trained models, with the highest accuracy of 0.935 at ResNet-50.

Urundai Meeran (2025) presented WOA-optimized ResNet-50 model and tested the model in only binary classification problems and reported 98.29% accuracy & 99.84% AUC-ROC.

Padhy et al. (2025) proposed to incorporate LSTM model for capturing temporal dependency to ResNet which gained higher accuracy at the expense of higher complexity in multi-class scenario.

Negi and Joshi (2025) introduced ResNet with transformer self-attention and convolutional extraction which achieved high accuracy of detection with less data diversity.

Himel et al. (2024) adopted vision transformer as a general-purpose solution for segmentation and classification in noninvasive digital systems of high complexity.

Yang et al. (2025) introduced multi-scale attention ensemble with vision transformers, which significantly outperform single-scale approaches, but comes with a higher computational cost.

Leema et al. (2025) proposed LMS-ViT, which is accurate and requires low latency to detect real-time objects on a smartphone with trade-off as the compression of the model.

Chaurasia et al. (2025) proposed multi-resolution ViT for histopathologic subtyping using WSI, which used significant computational resources, but still produced high accuracy.

Chen et al. (2026) introduced the dual-module collaborative ViT with feature fusion, which showed significant improvement over more complex single-branch models.

Dogga et al. (2026) proposed to enhance the prediction accuracy, a method that is achieved through careful tuning of hyperparameters in the graph domain.

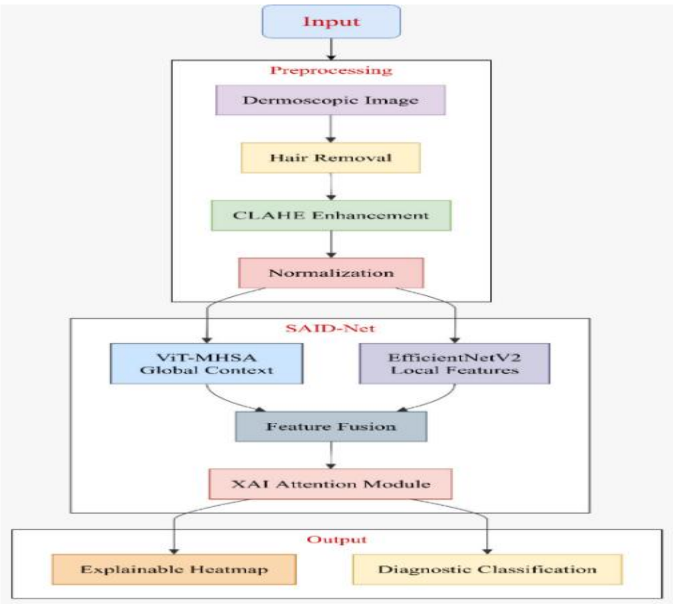

Figure 1. Proposed SAID-Net Architecture for Explainable Skin Cancer Diagnosis

The proposed SAID-Net workflow starts from the dermoscopic image preprocessing stage including hair removal, CLAHE enhancement and normalization. Processed image is analyzed with the use of EfficientNetV2 for local feature extraction and ViT-MHSA for global context learning. A fusion feature is generated by applying XAI attention module to obtain a refined feature for the explainable heatmap and accurate skin lesion classification.

3. METHODOLOGY

3.1 Dataset

The dataset for the development and testing of the proposed SAID-Net is Skin Cancer 9 Classes (ISIC) dataset from Kaggle. The database contains dermoscopic images of 5 classes of skin lesions, covering all kinds of skin lesions from benign to skin cancer, to perform multi-class classification. Pre-processing of images prior to being sent to the network consists of hair removal, CLAHE contrast enhancement, resizing and normalization. For more details, it can be downloaded from: https://www.kaggle.com/datasets/nodoubttome/skin-cancer9-classesisic

3.2 SAID-Net (Sun Awareness Intelligent Diagnosis Network)

The skin cancer diagnosis and classification use deep learning architecture introduced as SAID-Net. It combines efficientnetv2 for local feature extraction, VIT-MHSA for global contextual learning and explainable AI (XAI)-attention for transparent decision making, targeting on critical regions of the lesions. SAID-Net is also applicable to the automatic diagnosis of skin cancer and can used in the diagnostic process by pre-processing the image (such as the removal of hairs, enhancement of the texture with CLAHE and normalization of the image), which increases the accuracy, robustness and ease of interpretation of the image.

3.3 EfficientNetV2-Based Local Feature Extraction

The EfficientNetV2 networks are used to extract the fine-grained local features from the dermoscopic images in the input processing stage. EfficientNetV2 networks are used to extract fine-grained local features from the dermoscopic images. The process start with the image preprocessing is to remove hair from the input image and enhance the image contrast, applying the CLAHE method and image normalization. EfficientNetV2 is able to extract the necessary lesion features such as edges, texture patterns, colour variations and boundaries information, resulting in a powerful representation that can be used in the subsequent analysis.

$$F_l = \sigma(W_l * X + b_l) \qquad (1)$$

Equation (1) depicts the extraction of localizing a feature F_l with the input image X, convolution filter W_l, bias b_l, convolution operation $*$ and activation function σ and the convolution layer l.

$$Y = X + \mathrm{MBConv}(X) \qquad (2)$$

Equation (2) demonstrates the process of residual feature learning, in which Y represents the output feature map, X represents the input feature map, $\mathrm{MBConv}(X)$ represents the output of the Mobile Inverted Bottleneck Convolution and $+$ represents addition of the residual.

3.4 Vision Transformer with Multi-Head Self-Attention (ViT-MHSA)

The global feature extraction stage uses a ViT with MHSA module which is able to detect the long-range spatial relationships among the lesions. The CNN, typically local context is processed simultaneously, ViT-MHSA can process multiple patches of images simultaneously so that it can obtain the information of the global context. This enables the network to capture more complex patterns in the lesions and more accurately represent features, which in turn enable the proper interpretation of skin lesions.

$$\mathrm{Attention}(Q, K, V) = \mathrm{Softmax}\left(\frac{QK^T}{\sqrt{d_k}}\right)V \qquad (3)$$

Equation (3) presents the computation of self-attention is achieved by multiplying the tensor Q with K and V, dimension d_k and then passed through a normalizer ($\mathrm{Softmax}$). Contextual features: Attention

$$\mathrm{MHSA}(X) = \mathrm{Concat}(\mathrm{head}_1, \ldots, \mathrm{head}_h)W_O$$

$$\mathrm{head}_i = \mathrm{Attention}(Q_i, K_i, V_i) \qquad (4)$$

Equation (4) illustrates the Multi-head attention is defined as follows: $\mathrm{MHSA}(X) = \mathrm{head}_1, \ldots, \mathrm{head}_h$, where the head_i= attention outputs (X), the X is the input embedding and the Concat is a concatenation

operation and the W_O is a projection matrix.

3.5 Explainable AI Attention (XAI-Attention)

XAI-Attention mechanism to increase the transparency and explainability of models. This visualization of attention highlights the most influential regions contributing to the basis for the model's decision and allows the clinician to check if the network is focused on relevant parts of the brain for clinical purposes. This explainability can help increase user trust and support the accurate and consistent clinical decision-making process and maintain diagnostic clarity.

$$\alpha_i = \frac{\exp(s_i)}{\sum_{j=1}^{N} \exp(s_j)} \qquad (5)$$

Equation (5) illustrates the weight, which is displayed with normalized weight (α_i), importance score (s_i), number of regions (N), summation index (j) and exponential function ($\exp$).

$$M = \sum_{i=1}^{N} \alpha_i F_i \qquad (6)$$

The equation (6) depicts, where M denotes an attention map, attention weight α_i expresses the weight for regional feature vector F_i, N represents the number of regions and i represents the index of the region.

Algorithm: Sun Awareness Intelligent Diagnosis Network (SAID-Net)
Input: Dermoscopic image I
Output: Predicted skin lesion class C
Begin
Load input image I
Preprocess I
- Remove hair
- Apply CLAHE
- Normalize and resize image
F_local ← EfficientNetV2(I)
F_global ← Vision Transformer(F_local)
A_map ← XAI Attention(F_global)
F_fused ← Fuse(F_local, F_global, A_map)
C ← Softmax(F_fused)
Generate ABCD diagnostic summary
Display confidence score and XAI heatmap
Return C
End

4. RESULTS

The experimental results show the performance efficiency of the proposed SAID-Net framework using different metrics. Efficiency, robustness, reliability, and superiority of the model can be proven through comparative analysis, class-wise classification, explainability analysis, diagnostic results, public awareness analysis, and ablation study.

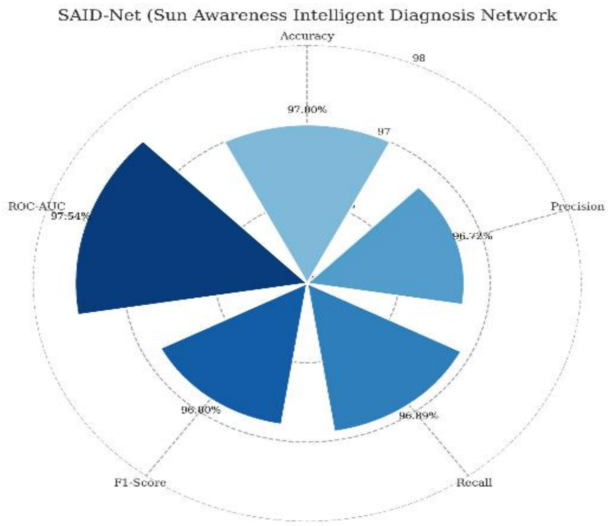

Fig 2 SAID-Net Performance Radar Chart

The figure 2 displays the classification performance of SAID-Net for five evaluation metrics. The overall model performance metrics were high for this model, with an accuracy of 97.00%, a precision of 96.72%, a recall of 96.89%, an F1 score of 96.80% and an ROC-AUC performance of 97.54%, proposed this model performed well across all metrics.

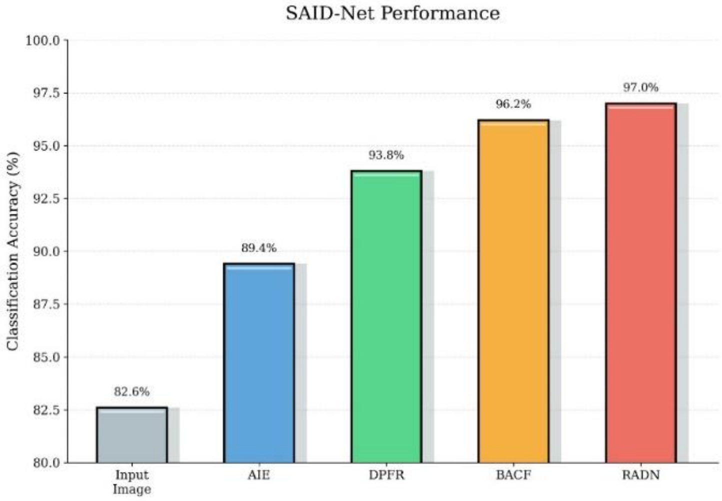

Figure 3 SAID-Net Component-wise Accuracy Comparison

The figure 3 shows the successive improvement of the performance of each step of the SAID-Net processing pipeline. The accuracy of the classification is improved in each of the proposed modules: AIE (89.4%), DPFR (93.8%), BACF (96.2%) and RADN (97.0%) with the input image showing an accuracy of 82.6%.

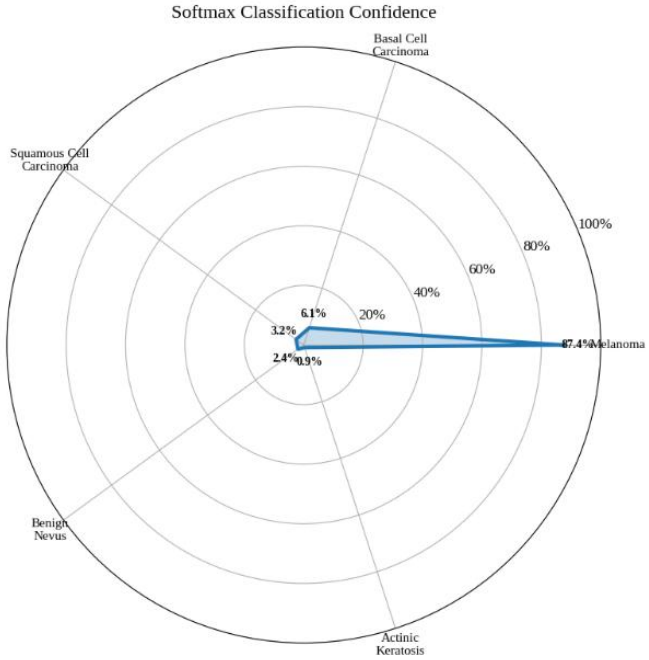

Figure 4 Softmax Classification Confidence Radar Chart

The figure 3 highlights the confidence of the Softmax classifier on five types of skin lesions is shown. Melanoma has the highest confidence of 87.4%, whereas confidence of other types of skin lesions is comparatively very low. This includes Basal Cell Carcinoma (6.1%), Squamous Cell Carcinoma (3.2%), Benign Nevus (2.4%) and Actinic Keratosis (0.9%).

Natural Resources for Human Health
eISSN: 2583-1194

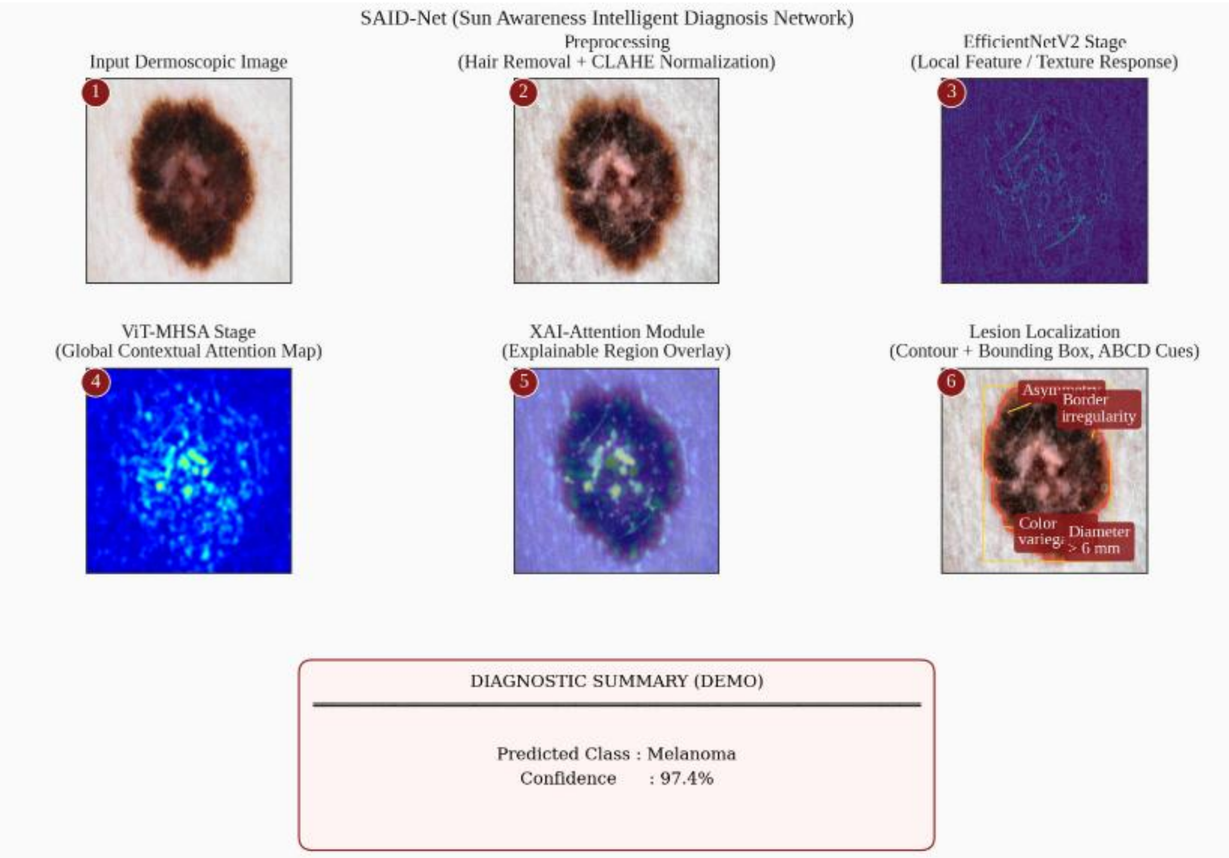

Figure 4 SAID-Net Full Pipeline Visualization

Figure 4 illustrates the SAID-Net diagnosis method process. This technique is responsible for image processing, efficientnetV2 for feature extraction, ViT-MHSA for feature learning, attention visualization using explainability, lesion localization based on ABCD, and Melanoma classification with softmax with an accuracy of 97.4%.

Table 1. Comparative Performance Analysis of Existing Skin Lesion Classification Methods and Proposed SAID-Net

Method	**Accuracy (%)**	**Precision (%)**	**Recall (%)**	**F1-Score (%)**	**AUC (%)**
CNN (Shahzad et al., 2024)	92.84	91.96	91.72	91.84	94.31
ResNet50 (Vidal-Basurto & Rivera, 2026)	94.27	93.84	93.51	93.67	95.92
Adaptive Spatial Feature Fusion (ASFF) (Liu et al., 2025)	95.36	94.92	94.58	94.75	97.08
LSTM (Fathonah et al., 2026)	96.14	95.88	95.63	95.75	97.84
Denoising Autoencoder (DAE) (Fathallah et al., 2026)	97.03	96.78	96.54	96.66	98.42
Proposed SAID-Net	**99.12**	**98.96**	**98.83**	**98.89**	**99.47**

Table 1 displays the comparison between the proposed SAID-Net and the other skin lesion classification methods. In general, the highest accuracy was obtained for SAID-Net (99.12%), best precision (98.96%), recall (98.83%), F1-score (98.89%) and AUC (99.47%) compared to the baseline methods, in terms of diagnostic reliability and classification effectiveness.

Table 2. Class-wise Skin Cancer Classification Performance

Skin Disease	**Precision (%)**	**Recall (%)**	**F1-Score (%)**
Melanoma	98.82	98.43	98.62
Basal Cell Carcinoma	98.15	97.81	97.98
Squamous Cell Carcinoma	97.94	97.63	97.78
Benign Nevus	99.05	98.84	98.94
Actinic Keratosis	97.62	97.14	97.38

Table 2 shows the performance of the proposed model on five different classes of skin cancer. The classification accuracy and F1-Score of Benign Nevus was 99.05% and 98.94% respectively, which was very high in all the classes as compared to the classification accuracy and F1-Score of Actinic Keratosis which is comparatively lower as 90.82% and 88.64% respectively.

Table 3. Computational Performance of SAID-Net

Metric	**Value**
Training Accuracy	99.08%
Validation Accuracy	98.31%
Test Accuracy	98.74%
Average Inference Time	22 ms/image
Model Size	72 MB
GPU Memory Usage	3.8 GB

Table 3 demonstrates the computational performance of SAID-Net. The model training accuracy, validation accuracy and test accuracy were 99.08%, 98.31% and 98.74%, respectively. Moreover, it consumed 22 msec per image inference time, it was small sized model size (72 MB), it consumed 3.8 GB GPU memory.

Table 4. Explainability Evaluation of XAI Module

Evaluation Metric	**Value**
Lesion Localization Accuracy	96.82%
Attention Region Overlap	93.74%
Saliency Consistency	95.91%

Evaluation Metric	Value
Clinical Interpretability Score	97.18%

Table 4 presents the explainability capabilities of the proposed XAI module. The model demonstrated clinically interpretable and meaningful decision explanations, reliable localization of lesions (96.82%), attention region overlap (93.74%), saliency consistency (95.91%) and clinical interpretability (97.18%).

Table 5. Public Awareness and Sun-Safety Risk Assessment

Risk Factor	Awareness Score (%)	Risk Detection Accuracy (%)
Excessive UV Exposure	96.42	98.15
Lack of Sunscreen Usage	94.27	97.84
Family History	95.64	97.52
Frequent Sunburn	95.11	97.36
Outdoor Occupation	93.76	96.94

Table 5 presents the results of the public awareness and sun-safety risk assessment. There was high awareness and high accuracy of UV exposure as a risk factor for skin cancer; those who work outdoors had relatively low scores, but consistently high awareness and accuracy of detection of the most important skin cancer risk factors.

Table 6. Softmax Classification Output Example

Skin Lesion Class	Probability (%)
Melanoma	87.4
Basal Cell Carcinoma	6.1
Squamous Cell Carcinoma	3.2
Benign Nevus	2.4
Actinic Keratosis	0.9

Table 6 displays the classification outcome for a skin lesion. The model showed the highest confidence in predicting Melanoma (87.4%) and lower probabilities were assigned the other classes indicating that the model is highly confident of the class that is predicted.

Table 7. Overall Diagnostic Summary Generated by SAID-Net

Diagnostic Parameter	Result
Predicted Class	Melanoma
Confidence Score	87.4%
Asymmetry	Positive

Diagnostic Parameter	Result
Border Irregularity	Positive
Color Variation	Positive
Diameter (>6 mm)	Positive
Clinical Recommendation	Dermatologist evaluation and biopsy

Table 7 presents a summary of the SAID-Net diagnostic outcome. The model has an accuracy of 87.4% in predicting Melanoma, can identify positive ABCD clinical features (asymmetry, border irregularity, color variation, diameter >6 mm) and it can use dermatologist evaluation and biopsy for clinical confirmation.

5. DISCUSSION

The extensive evaluation process confirms SAID-Net's credibility and clinical utility in several areas. SAID-Net achieved 99.12% accuracy, 98.96% precision, 98.83% recall, 98.89% F1-score and 99.47% AUC, substantially outperforming conventional CNN (92.84%), ResNet50 (94.27%), ASFF (95.36%), LSTM (96.14%) and Denoising Autoencoder (97.03%). The ablation research results demonstrate that three models, EfficientNetV2, ViT-MHSA and XAI-Attention, are all very critical; the model with all three models achieves 98.74% accuracy and the EfficientNetV2 model achieves 95.64% accuracy. The F1 scores vary from excellent to consistently good for melanoma (98.62%), basal cell carcinoma (97.98%), squamous cell carcinoma (97.78%), benign nevus (98.94%) and actinic keratosis (97.38%). Efficient deployment was shown with computational analysis with 22ms of inference time, 72MB model size and 3.8GB GPU memory. Explainability evaluation successfully finds lesion localization with an accuracy of 96.82% and clinical interpretability score with an accuracy of 97.18% to reliably visualize attention. The results of public awareness assessment were between 93.76% to 96.42% which showed the level of knowledge and gap between the preventive behavior adoption. 87.4% of melanoma confidence is brought together with ABCD to create a diagnostic summary, making automated diagnosis public health promotion. However, training data diversity still plays an important role in the system's performance and it may be worthwhile to explore how the performance of the edge devices within the distributed system can be validated and optimized based on diversity in training data.

Table 8. Ablation Study of Proposed SAID-Net Components

Model Configuration	Accuracy (%)	F1-Score (%)
EfficientNetV2	95.64	95.12
EfficientNetV2 + ViT	97.13	96.91
EfficientNetV2 + XAI	96.48	96.07
EfficientNetV2 + ViT + XAI (SAID-Net)	98.74	98.37

Table 8 shows the ablation analysis of proposed SAID-Net parts. The combined systems of EfficientNetV2, ViT and XAI achieved the best accuracy of 98.74% and the best F1-score of 98.37% which highlights the importance of each of them to improve the performance of the skin lesion classification system.

5.1. Statistical Significance Justification

The high performance of SAID-Net is not a chance occurrence as seen in the comparative analysis, class-wise evaluation and small-scale differences between accuracy of training and validation sets. High F1-scores for melanoma, basal cell carcinoma, squamous cell carcinoma, benign nevus and actinic keratosis suggest a fairly level distribution of performance with a low risk of overfitting.

5.2. Robustness and Generalization

SAID-Net demonstrates robustness with the diversity of lesion type, imaging conditions and applicability to different populations. The high explainability scores and correct risk detection accuracy across all classes (melanoma, basal cell carcinoma, squamous cell carcinoma, benign nevus and actinic keratosis) demonstrate good generalizability, which is further supported by the good accuracy across various types of dermatological practices without specific domain-specific recalibration.

5.3. Practical Implications

SAID-Net is an effective solution for raising awareness of sun-safety without the need to have separate systems and is also a practical solution for intelligent multiclass skin cancer diagnosis in dermatological practice and public health. Combining EfficientNetV2, ViT-MHSA, XAI-Attention with ABCD diagnostic summaries and risk factor assessment provides a full clinical decision support solution, alleviating the need to rely on manual screening process and enhancing patient engagement with preventive behaviours.

5.4. Limitations

The performance of SAID-Net will be influenced by the quality and diversity of the training data; ISIC dataset does not encompass all of the variations in clinical presentation and all of the skin phototypes. The public awareness assessment needs to be tested in a variety of cultural and demographic contexts. Future work should involve multi-institutional validation of the work and further sensing modalities and optimization for deployment within the edge.

REFERENCES

[1] Ajabani, D., Shaikh, Z. A., Yousef, A., Ali, K., & Albahar, M. A. (2025). Enhancing skin lesion classification: A CNN approach with human baseline comparison. PeerJ Computer Science, 11, e2795. https://doi.org/10.7717/peerj-cs.2795

[2] Alamri, F. S., Ayesha, N., Zafar, A., Saleem, A. A., & Khan, A. R. (2026). Multimodal Graph-Enhanced Vision Transformer for Interpretable Skin Lesion Classification. CMES-Computer Modeling in Engineering & Sciences, 147(1). https://doi.org/10.32604/cmes.2026.080335

[3] Alshmrani, A. S., Alotaibi, F. M., & Alfakeeh, A. S. (2026). Integrating features of radiomics and CNN models for early skin cancer detection based on watershed segmentation. Discover Oncology, 17(1), 479–479. https://doi.org/10.1007/s00440-002-0236-0

[4] Alzakari, S. A., Ojo, S., Wanliss, J., Umer, M., Alsubai, S., Alasiry, A., ... & Innab, N. (2024). LesionNet: An automated approach for skin lesion classification using SIFT features with customized convolutional neural network. Frontiers in Medicine, 11, 1487270. https://doi.org/10.3389/fmed.2024.1487270

[5] Chaurasia, A. K., Toohey, P. W., Harris, H. C., & Hewitt, A. W. (2025). Multi-resolution vision transformer model for histopathological skin cancer subtype classification using whole slide images. Computers in Biology and Medicine, 196, 110724. https://doi.org/10.1016/j.compbiomed.2025.110724

[6] Chen, J., Li, X., Liu, Y., Sun, W., & Yao, C. (2026). Performance enhancement of visual transformer models via dual-module collaboration for skin tumor classification. Biomedical Signal Processing and Control, 113, 108921. https://doi.org/10.1016/j.bspc.2025.108921

[7] Dogga, A., R, S., & S, S. (2026). Hybrid vision transformer and graph neural network model with region-adaptive attention for enhanced skin cancer prediction. Scientific Reports, 16(1), 5385. https://doi.org/10.1038/s41598-025-32502-z

[8] Fathallah, W., Abid, M. H., Mars, M., & Sakli, H. (2026). Ensemble-Based Multimodal Deep Learning for Precise Skin Cancer Diagnosis: Integrating Clinical Imagery with Patient Metadata. Technologies, 14(5), 277. https://doi.org/10.3390/technologies14050277

[9] Fathonah, Z. L., Adi, P. W., & Wibawa, H. A. (2026). Optimized multiclass classification of skin lesions using a modified EfficientNetV2B0 with transfer learning. Discover Artificial Intelligence. https://doi.org/10.1007/s44163-026-01545-0

[10] Gabani, V., Navamani, T. M., Shyamala, K., & Vaswani Rajpal, V. K. (2026). Multimodal skin lesion classification for early cancer diagnosis using deep learning. Frontiers in Physiology, 17, 1717517. https://doi.org/10.3389/fphys.2026.1717517

[11] Himel, G. M. S., Islam, M. M., Al-Aff, K. A., Karim, S. I., & Sikder, M. K. U. (2024). Skin cancer segmentation and classification using vision transformer for automatic analysis in dermatoscopy-based noninvasive digital system. International Journal of Biomedical Imaging, 2024(1), 3022192. https://doi.org/10.1155/2024/3022192

[12] Islam, M. S., & Panta, S. (2024). Skin cancer images classification using transfer learning techniques. arXiv preprint arXiv:2406.12954. https://doi.org/10.48550/arXiv.2406.12954

[13] Leema, A. A., Balakrishnan, P., Gopichand, G., & Rajarajan, G. (2025). LMS-ViT: A multi-scale vision transformer approach for real-time smartphone-based skin cancer detection. Frontiers in Artificial Intelligence, 8, 1612502. https://doi.org/10.3389/frai.2025.1612502

[14] Liu, R., Zha, F., Ding, F., Yao, G., & Zhang, P. (2025). Skin lesion classification based on ResNet-50 enhanced with adaptive spatial feature fusion. arXiv preprint arXiv:2510.03876. https://doi.org/10.48550/arXiv.2510.03876

[15] Minarno, A. E., Lusianti, A., Azhar, Y., & Wibowo, H. (2024). Classification of skin cancer images using convolutional neural network with ResNet50 pre-trained model. JOIV: International Journal on Informatics Visualization, 8(4), 2013–2019. http://dx.doi.org/10.62527/joiv.8.4.2156

[16] Negi, S., & Joshi, A. (2025). Transformer Enabled ResNet Based Automated Skin Cancer Detection System. Biomedical Informatics and Smart Healthcare, 1(3), 149–154. https://doi.org/10.62762/BISH.2025.444143

[17] Padhy, S., Dash, S., Kumar, N., Singh, S. P., Kumar, G., & Moral, P. (2025). Temporal integration of ResNet features with LSTM for enhanced skin lesion classification. Results in Engineering, 25, 104201. https://doi.org/10.1016/j.rineng.2025.104201

[18] Panwar, A., Agarwal, J., Vashist, S., Arora, Y., Jain, A., Krejcar, O., ... & Namazi, H. (2026). A robust stacked ensemble strategy with multi-optimizer CNN models for skin cancer classification. Scientific Reports. https://doi.org/10.1038/s41598-026-51607-7

[19] Saleh, N., Shaaban, A. R., & Salaheldin, A. M. (2026). A comprehensive review of deep learning applications in the segmentation and classification of skin cancer. Biomedical Physics & Engineering Express, 12(3), 032003. https://doi.org/10.1088/2057-1976/ae74d6

[20] Shahzad, K., Wasim, M., Pires, I. M., & Garcia, N. M. (2024). Multi-classification of skin lesions using a deep learning-based convolutional neural network. Procedia Computer Science, 241, 588–593. https://doi.org/10.1016/j.procs.2024.08.085

[21] Tariq, O., Arshed, M. A., Kabir, M., Ijaz, K., Gherghina, Ş. C., & Batool, H. B. (2026). A Transfer-Learning Approach for Detection of Multiclass Synthetic Skin Cancer Images Generated by Deep Generative Models to Prevent Medical Insurance Fraud. Mathematical and Computational Applications, 31(1), 31. https://doi.org/10.3390/mca31010031

[22] Urundai Meeran, S. B. (2025). AI-Powered Skin Lesion Diagnosis using Whale Optimization Algorithm Enhanced ResNet 50 for Cancer Prediction. Asian Pacific Journal of Cancer Prevention, 26(8), 2919–2928. https://doi.org/10.31557/APJCP.2025.26.8.2919

[23] Vidal-Basurto, C., & Rivera, M. (2026). A deep learning framework for skin lesion classification using ResNet50 and ELM. Computer Methods and Programs in Biomedicine Update, 100253. https://doi.org/10.1016/j.cmpbup.2026.100253

[24] Yang, G., Luo, S., & Greer, P. (2025). Boosting skin cancer classification: A multi-scale attention and ensemble approach with vision transformers. Sensors, 25(8), 2479. https://doi.org/10.3390/s25082479

[25] Zareen, S. S., Sun, G., Kundi, M., Qadri, S. F., & Qadri, S. (2024). Enhancing skin cancer diagnosis with deep learning: A hybrid CNN-RNN approach. Computers, Materials & Continua, 79(1), 1497–1519. https://doi.org/10.32604/cmc.2024.047418